Physico–chemical characterization and sources of the thoracic fraction of road dust in a Latin American megacity

Omar Ramírez[a,b*], A.M. Sánchez de la Campa[a,c], Fulvio Amato[d], Teresa Moreno[d], Jesús D. de la Rosa[a,c]

[a] "Atmospheric Pollution" Associate Unit, CSIC–University of Huelva Centre for Research into Sustainable Chemistry–CIQSO, University of Huelva, Campus de El Carmen s/n, 21071, Huelva, Spain.
[b] Department of Civil and Environmental, Universidad de la Costa, Calle 58 #55–66, 080002, Barranquilla, Colombia.
[c] Department of Earth Sciences, University of Huelva, Campus de El Carmen s/n, 21071, Huelva, Spain.
[d] Institute for Environmental Assessment and Water Research (IDÆA), Spanish National Research Council (CSIC), C/Jordi Girona 18–26, Barcelona, Spain.

[*] Corresponding author. E–mail address: oramirez@cuc.edu.co, omar.ramirez@unad.edu.co

Abstract

Bogota is a Latin American megacity with frequent episodes of poor air quality due to high PM_{10} levels. Road dust has been identified as one of the main sources of this pollutant in the city, but there are no studies that have analyzed the physicochemical characteristics and origins of its respirable fraction. A characterization of inorganic compounds and an analysis of sources of the PM_{10} fraction of road dust was carried out in this study. A total of twenty road dust samples, selected from representative industrial, residential and commercial areas, were swept and resuspended to obtain the thoracic fraction. Organic carbon (OC), elemental carbon (EC), water soluble compounds, major elements and trace metals were analyzed. Size distribution by laser diffraction and individual particle morphology by Scanning Electron Microscopy (SEM) were also evaluated. The data obtained revealed that the volume (%) of thoracic particles was higher in samples from industrial zones where heavy vehicle traffic, industrial emissions and deteriorated pavements predominated. Crustal elements were the most abundant species, accounting for 49–62% of the thoracic mass, followed by OC (13–29%), water-soluble ions (1.4–3.8%), EC (0.8–1.9%) and trace elements (0.2–0.5%). The Coefficient of Divergence (CoD) was obtained to identify the spatial variability of the samples. A source apportionment analysis was carried out considering the variability of chemical profiles, enrichment factors and ratios of Fe/Al, K/Al, Ca/Al, Ti/Al, Cu/Sb, Zn/Sb, OC/TC and OC/EC. By means of a PCA analysis, five components were identified, including local soils and pavement erosion (63%), construction and demolition activities (13%), industrial emissions (6%), brake wear (5%) and tailpipe emissions (4%). These components accounted for 91% of the total variance.

Keywords

PM_{10}; Non–exhaust emissions; Bogota; Chemical composition; Resuspension; SEM

1. Introduction

Human exposure to PM_{10} (thoracic particles) is considered one of the main global health risk factors (WHO, 2016; IHME, 2017). This pollutant has been associated with cardiovascular diseases and strokes (Burnett et al., 2014; Du et al., 2016), and has also been linked to lung diseases (Song et al., 2014; Int–Panis et al., 2017), adverse outcomes at birth (Ha et al., 2014), allergies in children (Lee et al., 2014), diabetes (Pearson et al., 2010), asthma (Weinmayr et al., 2010), osteoporosis (Prada et al., 2017), oxidative stress induced by heavy metals (Ma et al., 2015) and cognitive impairment (Kioumourtzoglou et al., 2016; Chen et al., 2017). Exposure to thoracic particles is especially serious in densely populated cities where residents are constantly exposed to multiple anthropogenic sources, including emissions associated with road traffic. Although air pollution due to high PM levels is a characteristic phenomenon in urban contexts (Grobéty et al., 2010; Gulia et al, 2015), it is more common in megacities in developing countries (Gurjar et al., 2010; Ma and Jia, 2016; Ramírez et al., 2018a; Wheida et al., 2018). This has been observed in Latin America, where 77% of the population live in urban areas that do not comply with air quality standards, including PM_{10} levels (PAHO, 2005). Consequently, more than 100 million people are exposed to levels of air pollution above the guidelines recommended by the World Health Organization (Cifuentes et al., 2005; Green and Sanchez, 2013). This figure could increase in the coming years as an urban population of 570 million people has been projected in Latin America by 2025 (CEPAL, 2005).

Emissions related to road traffic represent a large contribution to the total concentrations of airborne particulate matter in urban areas (Thorpe and Harrison, 2008; Pant and Harrison, 2013). Vehicles emit primary particles and precursor gases of secondary particles (Perez et al., 2010; Calvo et al., 2013). Exhaust emissions include gases and fine/ultrafine carbon particles with small amounts of ions and metals (Zn, Pb, Cu, Ba, Cd, Cr, As) attributed to fuel and lubricant combustion (Gent et al., 2009; Peltier et al., 2011; Pulles et al., 2012). They also include traces of K, Br and Cl from engine (Pacyna, 1998), and Pt, Pd and Rh from catalytic converters (Prichard and Fisher, 2012). In general, traffic emissions come from exhaust pipes (exhaust emissions), wear of metal parts and resuspension of particulate material (non–exhaust emissions).

Non–exhaust emissions (such as pavement abrasion, tire and brake wear, and particle resuspension) release traces of Sr, Zn, Sb, Cu, Mo, Ba, Cd, Cr, Mn, Fe, among others into the atmosphere (Gietl et al., 2010). Road dust is defined as the material deposited on road surfaces susceptible to resuspension, and comprises a wide variety of particles, including crustal elements, allergens and anthropogenic organic/inorganic compounds (Thorpe and Harrison, 2008; Shi et al., 2010). This type of dust constitutes a significant source of PM emissions when it is resuspended (Viana et al., 2008; Huang et

al., 2011; Wang et al., 2014; Pant et al., 2015). Nowadays, the study of non–exhaust emissions is a major concern in cities around the world, since their contributions of PM are similar or even higher than those of exhaust emissions (Amato et al., 2009a; Amato et al., 2014a), contributing mainly to PM_{10} concentration (Thorpe and Harrison, 2008; Grobéty et al., 2010).

Bogota (the capital of Colombia) is a Latin American megacity of over 8 million inhabitants (DANE, 2010) and one of the most densely populated tropical cities in the world (17,700 hab/km^2) (Demographia, 2018). This city registers poor air quality (IDEAM, 2016; UNEP, 2016) due mainly to the high concentrations of PM_{10} (SDA, 2017, 2016). Source apportionment studies (SDA, 2009; Vargas et al., 2012; Ramírez et al., 2018a), emission inventories (Pachón et al., 2018) and air quality modeling (Nedbor–Gross et al., 2018) have identified road dust as one of the main sources of PM_{10} in Bogota. After analyzing daily samples of PM_{10} collected during a continuous year, Ramírez et al. (2018a) found that 23% of the airborne PM_{10} mass could be attributed to road dust resuspension. This percentage is significant and is a consequence of the poor condition of roads, a lack of maintenance and road cleaning, the presence of unpaved streets and pavements, and high traffic densities. However, most of the research and regulation have focused on studying and controlling exhaust emissions, leaving aside non-exhaust emissions.

Few studies analyzing road dust have been carried out in Bogota. Using emission factors, some authors have indirectly estimated the total emission of PM_{10} accounted for by dust resuspension and paved and unpaved road wear (23,300±5,000 ton/year) (Beltran et al., 2012). These authors concluded that 86% of non-exhaust emissions of PM_{10} associated with traffic are due to the resuspension of road dust, 9% to tire and brake wear, and 5% to road surface wear. Other studies have calculated the PM_{10} emission factor for resuspended particles in unpaved roads and in roads under construction (7.8±0.5 g/VKT and 28±0.27 μg/m^2*s, respectively) (Méndez et al., 2017). Finally, some researchers have analyzed the concentration of heavy metals (Pb and Cu) in deposited sediments on road surfaces in several urban areas, showing that metal concentrations tend to increase during dry weather (29–40%) (Romero et al., 2015; Zafra et al., 2015).

Despite its detrimental effect on the air quality and well-being of its citizens, there is limited information about road dust in Bogota. Therefore, characterizing the sources and composition of urban road dust is important for planning appropriate strategies to reduce air pollution. The aim of this study is to expand the current knowledge of road dust in one of the biggest megacities in Latin America (Bogota), by analyzing chemical properties of samples taken in representative residential, industrial and commercial areas of this city.

2. Materials and methods

2.1. Study area

Bogota is located in the center of Colombia at 2,550–2,620 m above sea level (Eastern Cordillera of the Andes). The city has a total area of ~ 1,600 km^2, an urban area of ~ 420 km^2 and a projected population of 8.9 million inhabitants by 2025 (SDP, 2017). The area designated for residential, commercial and industrial use is approximately 188 km^2, 58 km^2 and 5.4 km^2, respectively. The industrial sector (manufacturing, chemical, food and beverages, metallurgy, among others) is located within the urban area, particularly in the west and south of the city. Some sites in the Eastern Hills, particularly south of the city, are used as quarries for the extraction of construction materials. The urban road network totals 13,971 lane–km, of which only 47% (6,567 lane–km) is in good conditions, while 44% (6,147 lane–km) is in bad or defective condition, and the remaining 9% (1,257 lane–km) is unpaved (CCA, 2017). The city registered 2.1 million private vehicles, 460,000 motorcycles, 50,000 taxis and 25,000 collective transport buses in 2016 (SDM, 2017).

The average annual temperature and precipitation are 14 °C and 840 mm/year, respectively (IDEAM, 2015a). Bogota does not have seasons, but records two rainy periods a year (March–May and October–November). The remaining months record inferior levels of precipitation, particularly between December and February, when there are higher temperatures and lower rainfall. Winds from NE–E and SE–E prevail (IDEAM, 2015b).

2.2. Sampling sites

A total of twenty sampling points were selected in representative industrial, residential and commercial areas of Bogota. The Simón Bolívar Park, considered the largest metropolitan park in the city, was included as a background reference point (Rf). This site provided information on an urban background soil with low direct influence of anthropogenic pollution sources. Table 1 shows the main characteristics of each of the sampling points and Figure 1 shows their location. An overall description of each of the sampled sites is presented in the Supplementary File.

Table 1. Description of sampling sites.

Category	Code	Location		Description	Date
		Latitude (N)	Longitude (W)		
Industrial	I1	4°41'47.01"	74°09'12.42"	Close to the International Airport. High volume of heavy vehicles . Surrounded by unpaved roads.	02/22/2015
	I2	4°39'1.99"	74°06'52.02"	Next to the city's main coach station. High volume of inter–municipal buses.	02/22/2015
	I3	4°42'02.82"	74°05'58.37"	Low traffic volume. Located ~100 m from main roads with high traffic volume.	12/30/2015
	I4	4°35'44.63"	74°08'44.12"	Located at the exit to the city, in front of a petrol station, at a crossing of two high traffic avenues (Av Boyacá and Autopista Sur).	01/02/2016

	I5	4°38'13.77"	74°06'16.11"	No public transport transit . Industrial background. Surrounded by unpaved streets.	02/18/2015
	I6	4°38'21.44"	74°07'14.57"	High volume of heavy vehicles (trucks and inter-municipal buses).	11/16/2015
Residential	R1	4°39'47.08"	74°06'45.99"	In front of construction works. No industrial influence. Located ~200 m from an avenue with high traffic volume .	11/16/2015
	R2	4°44'39.7"	74°02'31.2"	Pavement in poor condition. Transited by public buses.	02/23/2015
	R3	4°43'39.02"	74°06'00.96"	High traffic volume. Close to roads under repair.	12/30/2015
	R4	4°44'51.3"	74°01'54.5"	High traffic volume. No industrial influence.	02/23/2015
	R5	4°34'29.51"	74°08'06.18"	In front of urban park. High traffic volume, including buses.	01/02/2016
	R6	4°39'57.88"	74°07'48.52"	High traffic volume. Located next to a cycleway. No industrial influence.	11/16/2015
Commercial	C1	4°46'44.69"	74°02'29.68"	Located at the exit to the city. High volume of heavy vehicles (trucks and inter-municipal buses).	01/03/2016
	C2	4°35'04.4"	74°05'49.2"	High traffic volume. Located in front of the bus rapid transit system (Transmilenio).	02/24/2015
	C3	4°35'6.60"	74°06'20.21"	High volume of heavy vehicles. Industrial influence present, and roads under repair.	02/24/2015
	C4	4°39'47.10"	74°03'41.08"	In front of Transmilenio bus rappid transit system. High traffic volume.	12/30/2015
	C5	4°37'03.62"	74°09'00.38"	High volume of heavy vehicles (trucks and buses).	01/02/2016
	C6	4°37'39.83"	74°03'55.48"	High traffic volume (including buses). Close to a bus stop and construction works.	12/30/2015
	C7	4°36'52.75"	74°04'14.95"	Frequently transited by buses. Close to a bus stop.	01/03/2016
Reference (urban park soil)	Rf	4°39'24.75"	74°05'31.27"	In the middle of an urban park. The closest road is ~200 m away.	01/03/2016

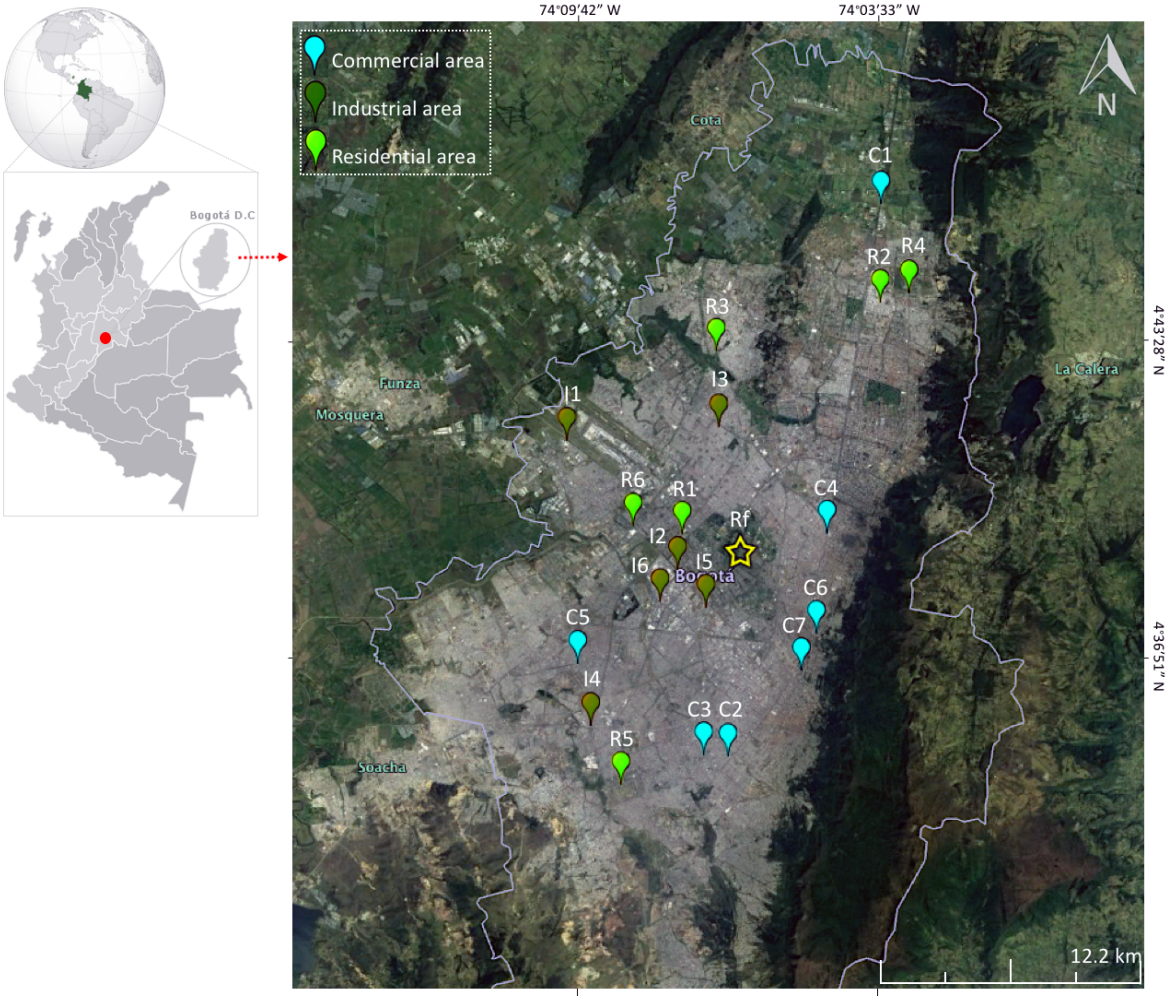

Fig. 1. Location of the sampling points grouped into three categories according to land use: industrial, commercial and residential areas. The Rf site is a reference point (urban park) with low direct traffic influence.

Sampling was carried out during the dry period between 2015 (February and November–December) and 2016 (January). Dust samples, of approximately 20–40 g, were collected directly from the right

side of traffic lane (kerbside) sweeping an area of 1 m^2 with plastic brushes and collectors (Quiroz et al., 2013; Pan et al., 2017). It was guaranteed that at the time of sampling no rain had been registered at least one week before. The samples were placed in clean sealed zip plastic bags (Apeagyei et al., 2011; Men et al., 2018) and then sent to the laboratory of the Institute for Environmental Assessment and Water Research (IDÆA) in Barcelona. A rotating closed drum was used under an air flow of 30 l/min to induce resuspension of dust and extract the thoracic fraction (< 10 μm). Each sample resuspended its finest fraction in the air space inside the drum with each rotation for 5 minutes, resulting in the resuspended aerosols being transported by the air stream from the drum to a quartz microfibre filter (MK 360, diameter 47 mm). The coarsest particles were deposited in the PVC chamber while the fraction below 10 μm was separated through an elutriation system. This equipment has been described in detail in previous studies (Moreno et al., 2007; Moreno et al., 2008).

2.3. Size distribution and morphological analysis

Raw samples of road dust were used for these analyses. The optical particle counter Mastersizer 2000 (Malvern) was used to calculate the size of the particles by measuring the intensity of the scattered light when a laser beam was passed through the sample. Its measurement range was between 0.02 to 2,000 μm, with a variation in accuracy and reproducibility below 1% (polydisperse standard), and a data acquisition speed of 1 kHz. This equipment incorporated a source of blue (low wavelenth) light for precise measurements in the submicron range. The analyses were carried out in triplicate and average particle size was calculated by D[4,3], that is equivalent diameter in terms of volume (Wua et al, 2009).

Scanning Electron Microscopy (SEM) provided additional direct information on grain size and shape of the road dust particles (Zhang et al., 2012), using the FEI Quanta 200 microscope. This is equipped with standard secondary electron and back scatter electron detectors, in addition to an energy dispersive X–ray analysis detector. The analytical conditions were 30 kV for the acceleration voltage and a working distance of 10 mm. The samples were covered with graphite.

2.4. Analytical methodology

Two PM_{10} filters were obtained from each site in order to collect enough samples for chemical analysis. Following a modified method proposed by Querol et al. (2008), half of the first filter was acid digested (HNO_3, HF, $HClO_4$), and the residue recovered with 5% HNO_3 in a Milli–Q H_2O solution. Major elements (Al, Fe, Mg, Ca, Na, S, K and P) and trace elements (V, Cd, Pb, Sr, Ba, Zn, Cu, Cr, As, Ni, Co, among others) were analyzed by ICP–OES (ULTIMA2 Jobyn Yvon) and ICP–MS (Agilent 7900), respectively. Silicon was estimated by stoichiometry using Al data (Querol et al.,

2001; Minguillón et al., 2014). The other half of the first filter was leached in 50 ml Milli–Q H_2O to determine the soluble fraction (SO_4^{2-}, Cl^-, NO_3^-, F^-, NO_2^-, Br^-, PO_4^{3-} and NH_4^+) by Ion Chromatography. A 4.6 cm^2 diameter portion of the second filter was analyzed for organic carbon (OC), elemental carbon (EC) and total carbon (TC = OC + EC) by a Thermal Optical Transmittance (TOT) method (Birch and Cary, 1996), using a carbon analyzer (Sunset Laboratory Inc.). The EUSAAR2 (European Supersites for Atmospheric Aerosol Research) protocol was followed (Cavalli et al., 2010) (Supplementary Table 1). The quality of the results was controlled by certified reference standards (NBS1633b). The average precision and accuracy were within normal analytical errors (5–10%).

2.5. Coefficient of Divergence (CoD)

The samples showed variations in their chemical profiles, making it necessary to use a standardization procedure, such as the CoD proposed by Wongphatarakul et al. (1998), to quantify the spatial variability. CoD has been used in several road dust studies (Fujiwara et al., 2011a; Kong et al., 2011; Samiksha et al., 2017) and is defined in Equation 1.

$$CoD_{AB} = \sqrt{\frac{1}{p}\sum_{i=1}^{p}(X_{Ai} - X_{Bi}/X_{Ai} + X_{Bi})^2} \qquad [1]$$

where X_{Ai} and X_{Bi} represent the concentration of the chemical component i in profiles A and B, respectively. A and B represent two profiles for comparative analysis, and p is the number of chemical species that were taken into account. In this study, CoD was calculated taking into consideration all of the analyzed species . If the CoD value approaches zero, the chemical profiles of A and B are highly similar, while a value approaching unity indicates high dissimilarity.

2.6. Enrichment factors

Enrichment factors (EFs) have been widely used to determine the degree of enrichment due to human activity in road dust, and separate probable natural from anthropogenic sources. EFs were calculated for the thoracic fraction of road dust using Equation 2 (Zoller et al., 1974).

$$EF_{[El]} = \frac{[El]_{sample}/[X]_{sample}}{[El]_{background}/[X]_{background}} \qquad [2]$$

where [*El*] is the concentration of element under consideration, [*X*] is the concentration of the chosen reference element, and the subscripts *sample* or *background* indicate which source the concentration refers to. In this study, the background source selected was the Rf site (urban park soil), in comparison with which the anthropogenic influence on the residential, commercial and industrial road dust was determined. The reference element chosen is often Al, Li, Sc, Zr or Ti (Reimann and de Caritat, 2005), or even Fe (Valotto et al., 2015) and Mn (Saeedi et al., 2012). We selected Al because it has been identified as suitable for terrestrial studies (Reimanna and de Caritat, 2005) and previous research has considered it appropriate for road dust studies given its low variability associated with traffic (Birmili et al., 2006; Pant et al., 2015; Samiksha et al., 2017). EF values > 1 typically indicate enrichment of the sample by anthropogenic sources, according to the following classifications: minimal (EF = 1–2), moderate (EF = 2–5), significant (EF = 5–20), very high (EF = 20–40) and extremely high (EF > 40) (Yongming et al. al., 2006; Mummullage et al., 2016).

3. Results and discussion

3.1. Size distribution of road dust particles

Following analysis of the raw samples of road dust, it was noted that the dust distribution patterns at the industrial, commercial and residential areas were similar. All three were characterized by a significant unimodal distribution, with most of the particles in the range of 50 to 300 μm (Fig. 2). The average size of the particles in the commercial area was 232±58 μm, in the industrial area 211±58 μm and in the residential area 190±98 μm. Anomalous variations and large particle sizes were observed (0.39–1,840 μm), which could have been due to the particles not being sifted previously. Possible urban sources of road dust include eroded soils, wear of pavement and vehicular parts, unpaved streets, construction works, and industrial emissions, among others.

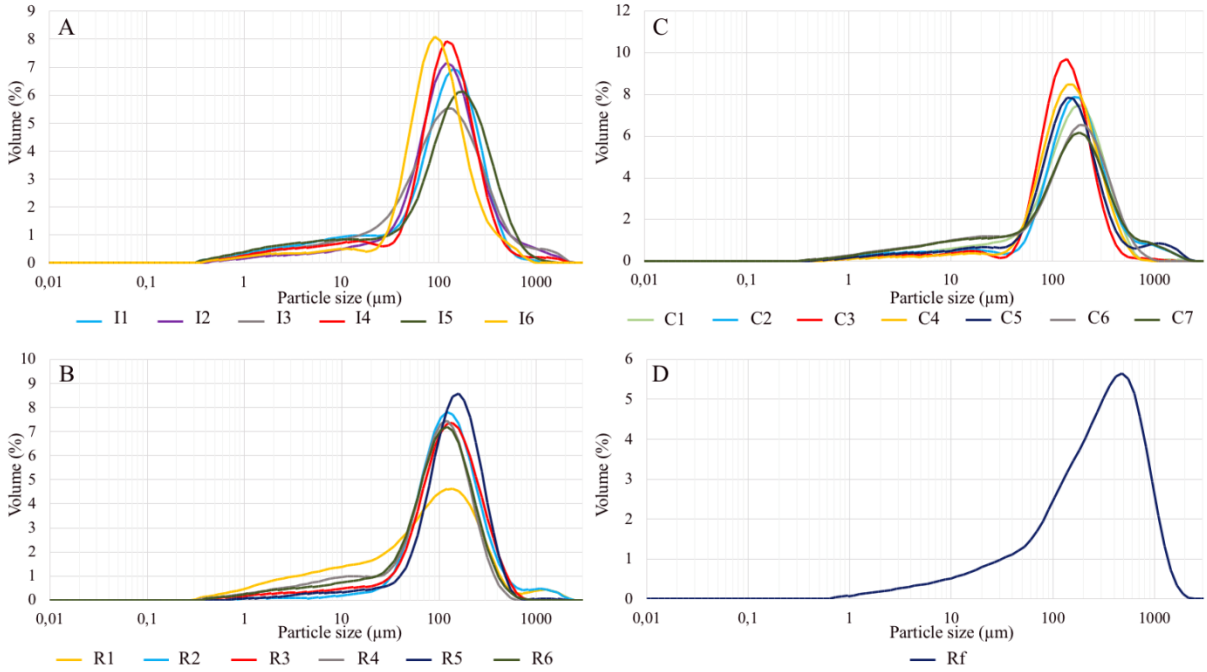

Fig. 2. Size distribution of road dust particles grouped by land use: A) industrial area, B) residential zone, C) commercial area, D) reference point (urban park soil).

Identifying the particle size distribution enables us to know the volume (%) of thoracic particles from road dust (PM_{10}) with the potential to be resuspended and inhaled (Shi et al., 2011). The results obtained indicate that the average percentage of thoracic fraction in industrial road dust was twice as high (10%) as that registered in the Rf (5%), while the residential and commercial road dust exceeded this by 1.8 (8.7%) and 1.6 times (7.8%), respectively. This indicates that the thoracic fraction from road dust was higher in industrial zones, where heavy vehicle traffic, industrial emissions and deteriorated pavements predominated. However, the invidual road dust sample with the highest percentage of PM_{10} (R1, 19%) was unexpectedly located in a residential area in front of construction works. This highlights the importance of this type of activity as sources of PM_{10} in Bogota, as has also been reported in European (Amato et al., 2014b) and Latin American cities (Fujiwara et al., 2011b). The thoracic fraction values obtained in our study were lower than those reported in Chinese cities, where on average 20% of particles in road dust contributed to the diameters < 10 µm (Shi et al., 2011).

3.2. Chemical profiles

Table 2 provides the profile of the major components and ions in the thoracic fraction of the four categories considered in this study. The standard deviation of the Rf was equated with the analytical error (5%).

Table 2. Chemical composition of major components in the thoracic fraction of road dust in four urban areas. Concentration in mass percentage (%). DL: detection limit. SD: standard deviation (analytical error for reference profile). Highest values for each variable are highlighted in bold.

Species	Residential (n=6)		Industrial (n=6)		Commercial (n=7)		Reference (Rf) (n=1)		Whole (n=20)	
	Mean	SD	Mean	SD	Mean	SD	Mean	SD	Mean	SD
EC	0.52	0.63	0.25	0.38	**1.94**	**0.70**	0.76	0.04	0.66	0.63
OC	12.7	5.75	14.3	6.94	19.4	7.07	**29.0**	**1.45**	14.7	7.79
Al	10.5	2.49	9.57	5.08	**11.6**	**4.89**	11.1	0.55	10.1	5.85
Si	27.7	6.59	25.3	13.4	**30.7**	**12.9**	29.3	1.46	26.7	15.5
Ca	**10.0**	**7.10**	5.99	2.64	8.37	3.47	2.99	0.15	7.73	6.86
Fe	4.30	1.83	4.66	1.98	6.25	2.50	**8.31**	**0.42**	4.85	2.49
K	1.13	0.58	1.35	0.65	**1.72**	**0.67**	1.23	0.06	1.31	0.77
Mg	0.67	0.21	0.62	0.25	**0.76**	**0.27**	0.59	0.03	0.65	0.77
Na	0.46	0.22	0.71	0.13	**1.15**	**0.50**	0.20	0.01	0.66	0.30
P	0.33	0.05	0.39	0.11	0.48	0.16	**0.50**	**0.03**	0.37	<0.01
S	0.47	0.36	0.41	0.16	**0.67**	**0.40**	0.35	0.02	0.48	0.35
Cl^-	0.06	0.06	0.04	0.03	0.21	0.04	**0.27**	**0.01**	0.09	0.05
F^-	0.04	0.02	0.01	<0.01	0.13	0.07	**0.20**	**0.01**	0.05	0.03
Br^-	0.43	<0.01	0.45	0.02	1.25	0.09	**1.61**	**0.08**	0.60	0.03
PO_4^{3-}	<DL	<DL	<DL	<DL	<DL	<DL	<DL	<DL	<DL	<DL
NO_2^-	0.06	0.01	0.07	0.02	0.05	0.01	<DL	<DL	0.07	0.03
NO_3^-	0.07	0.08	0.07	0.02	**0.08**	**0.07**	0.05	<0.01	0.07	0.07
SO_4^{2-}	0.74	0.32	0.62	0.14	**1.55**	**0.65**	<DL	<DL	0.89	0.35
NH_4^+	0.12	0.05	0.13	0.02	0.55	0.15	**1.15**	**0.06**	0.23	0.09

Averaging the concentrations of all the samples, the most abundant major components were Si (26.7±15.5%), OC (14.7±7.8%) and Al (10.1±5.9%), followed by Ca (7.7±6.9%), Fe (4.9±2.5%) and K (1.3±0.8%) (Table 2). The most abundant water-soluble ions were SO_4^{2-} (0.89±0.35%) and NH_4^+ (0.23±0.09%). Meanwhile, the most abundant trace elements were Ti, Ba and Zn, followed by Mn, Sr, Cu, Pb and Zr (Table 3). Table 3 lists twenty selected trace elements, all others being presented in Supplementary Table 2.

Table 3. Selected trace elements in the thoracic fraction of road dust in four urban areas. Concentration in ppm. SD: standard deviation (analytical error for reference profile). DL: detection limit. Highest values for each variable are highlighted in bold.

Species	Residential (n=6)		Industrial (n=6)		Commercial (n=7)		Reference (Rf) (n=1)		Whole (n=20)	
	Mean	SD	Mean	SD	Mean	SD	Mean	SD	Mean	SD
As	**0.0026**	**0.0016**	0.0016	0.0007	0.0007	0.0003	0.0006	0.0000	0.0015	0.0012
Cr	**0.0292**	**0.0095**	0.0251	0.0091	0.0116	0.0032	0.0062	0.0003	0.0207	0.0109
Cu	**0.0390**	**0.0166**	0.0353	0.0130	0.0283	0.0066	0.0042	0.0002	0.0324	0.0140
Mn	0.0870	0.0150	0.0738	0.0283	<DL	<DL	<DL	<DL	0.0785	0.0222
Ni	0.0098	0.0032	**0.0109**	**0.0058**	0.0053	0.0018	0.0029	0.0001	0.0082	0.0045
Pb	0.0356	0.0175	**0.0436**	**0.0046**	0.0144	0.0032	0.0080	0.0004	0.0292	0.0165
Sr	**0.1272**	**0.0877**	0.0594	0.0223	0.0295	0.0095	0.0156	0.0008	0.0671	0.0633
Ti	**1.0530**	**0.2648**	0.8429	0.3340	0.3841	0.1514	0.2732	0.0137	0.6992	0.3802
V	**0.0308**	**0.0129**	0.0207	0.0118	0.0094	0.0046	0.0061	0.0003	0.0190	0.0132
Zn	0.1558	0.0867	**0.2392**	**0.1650**	0.0899	0.0208	0.0316	0.0016	0.1515	0.1178
Li	**0.0080**	**0.0038**	0.0047	0.0025	0.0025	0.0012	0.0015	0.0001	0.0048	0.0034
Rb	**0.0124**	**0.0049**	0.0090	0.0049	0.0039	0.0018	0.0031	0.0002	0.0079	0.0052
Zr	**0.0305**	**0.0124**	0.0235	0.0156	0.0121	0.0041	0.0064	0.0003	0.0212	0.0136
Ba	**0.2316**	**0.0648**	0.2181	0.0827	0.0979	0.0339	0.0335	0.0017	0.1709	0.0900
La	**0.0162**	**0.0070**	0.0109	0.0050	0.0045	0.0023	0.0037	0.0002	0.0099	0.0068
Sc	**0.0029**	**0.0013**	0.0020	0.0011	0.0008	0.0004	0.0006	0.0000	0.0018	0.0013
Co	**0.0021**	**0.0012**	0.0017	0.0007	0.0007	0.0002	0.0004	0.0000	0.0014	0.0010
Cd	**0.0003**	**0.0002**	**0.0003**	**0.0001**	0.0001	0.0000	0.0001	0.0000	0.0002	0.0001
Sn	**0.0049**	**0.0026**	0.0034	0.0012	0.0025	0.0009	0.0004	0.0000	0.0034	0.0020
Sb	**0.0038**	**0.0020**	0.0029	0.0012	0.0034	0.0021	0.0005	0.0000	0.0032	0.0019

Chemical species were classified into major elements (including Si, Ti, Al, Mn, Mg, Ca, Fe, K, S and Na), trace elements (Cu, Zn, As, Pb, Cr, Ni, Co, Cd and V), water-soluble ions (SO_4^{2-}, Cl^-, NO_3^-, F^-, NO_2^-, Br^-, PO_4^{3-} and NH_4^+), OC and EC to compare the data obtained with other studies. Figure 3 shows the chemical compositions of each group.

Major elements were the most abundant species, accounting for 62±26% of PM_{10} mass in the commercial sector, 56±19% in the residential sector, 55±3% in Rf and 49±25% in the industrial area. These percentages were higher than those reported for road dust in Barcelona (~ 35%), roadsite dust in New Delhi (~ 25%) and road dust in Chinese cities such as Fushun (~ 30%) (Table 4). This could be associated with the poor state of the pavement, dust contribution from construction works and emissions from the quarries located within the urban area in Bogota. The values obtained were similar to those recorded in dust from heavily trafficked roads in Birmingham (~ 50%) and Gold Coast (~ 60%, Gunawardana et al., 2012), and road dust collected at building sites in Fushun (~ 50%).

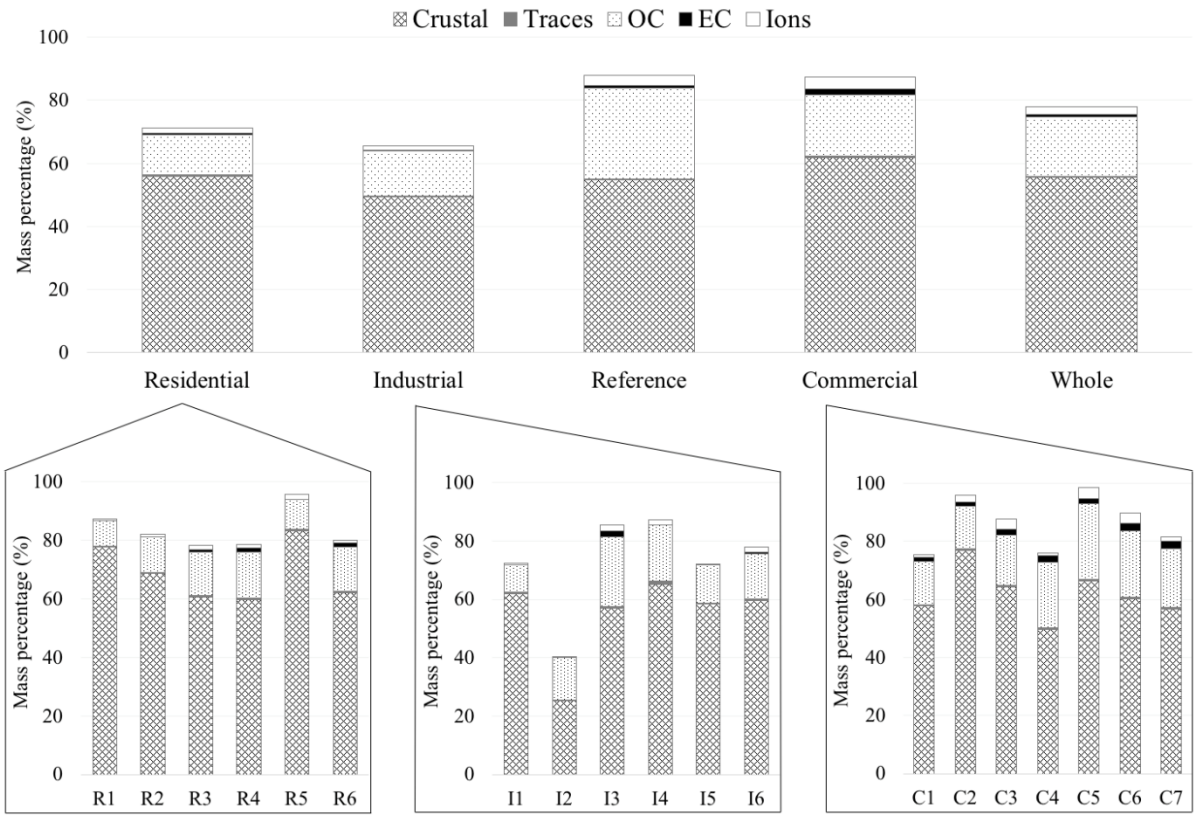

Fig. 3. Chemical profiles of the studied areas by land use in Bogota.

Table 4. Chemical profiles of the thoracic fraction from road dust in several cities. Concentration in %. NR: not reported. *Al_2O_3. **SiO_2

	Amato et al., 2009b			Kong et al., 2011		Pant et al., 2015	
	Barcelona			**Fushun**		**Birmingham**	**New Delhi**
	City center (n=8)	Ring roads (n=5)	Construction (n=4)	Road dust (n=30)	Construction (n=19)	Roadside (n=10)	Roadside (n=10)
OC	11.94±1.69	9.65±3.45	9.46±1.08	7.49±2.61	2.95±0.93	7.91±4.80	1.82±1.69
EC	2.92±1.62	1.81±1.84	1.34±0.57	5.74±1.89	2.49±0.99	0.13±0.41	0.51±0.29

Al	8.10±3.74*	8.91±1.39*	8.57±1.55*	6.53±3.26	6.59±2.22	8.66±4.81	3.98±1.04
Ca	13.09± 4.75	11.71±1.22	15.43±3.26	8.41±6.69	26.65±6.13	3.24±1.62	5.00±0.64
Fe	5.18±2.11	4.02±0.66	3.83±1.19	0.97±0.34	0.81±0.14	7.39±8.92	3.11±0.49
Mg	1.25±0.47	1.23±0.10	1.27±0.18	2.46±2.47	1.60±1.45	NR	NR
P	0.14±0.06	0.08±0.02	0.12±0.03	NR	NR	NR	NR
S	0.54±0.16	0.49±0.18	0.42±0.20	<0.001	<0.001	0.11±0.18	NR
Si	19.40±9.00**	21.40±3.34**	20.60±3.73**	9.25±4.20	12.11±1.60	28.80±17.60	13.00±3.04
Na	0.45±0.14	0.50±0.15	0.32±0.09	1.71±0.13	1.63±0.21	NR	NR
K	1.43±0.61	1.54±0.24	1.50±0.18	0.23±0.15	0.34±0.33	NR	NR
NO_3^-	0.29±0.32	0.13±0.07	0.04±0.03	0.07±0.07	0.01±0.01	NR	NR
SO_4^{2-}	1.37±0.84	1.01±0.61	0.77±0.78	0.27±0.22	0.22±0.14	NR	NR
Cl^-	0.54±0.32	0.22±0.13	0.19±0.17	0.09±0.32	0.01±0.02	NR	NR
NH_4^+	0.21±0.18	0.04±0.02	0.02±0.01	0.03±0.14	0.001±0.002	NR	NR
As	0.001±0.000	0.001±0.000	0.002±0.001	0.002±0.001	0.001±0.001	NR	NR
Cr	0.024±0.010	0.013±0.007	0.012±0.006	0.529±0.864	1.145±1.360	0.007±0.006	0.006±0.001
Cu	0.139±0.071	0.077±0.062	0.049±0.047	0.014±0.014	0.008±0.008	0.035±0.029	0.016±0.000
Mn	0.067±0.024	0.062±0.005	0.059±0.010	0.073±0.041	0.051±0.038	0.044±0.037	0.044±0.005
Ni	0.006±0.002	0.005±0.002	0.004±0.002	0.019±0.044	0.008±0.017	NR	NR
Pb	0.023± 0.010	0.023±0.015	0.018±0.003	0.007±0.007	0.006±0.008	NR	NR
Sr	0.024±0.007	0.021±0.003	0.028±0.005	NR	NR	NR	NR
Ti	0.288± 0.121	0.314±0.030	0.282±0.044	0.379±0.380	0.468±0.298	0.032±0.025	0.047±0.005
V	0.008±0.003	0.010±0.001	0.001±0.002	0.002±0.000	0.009±0.034	0.002±0.002	0.003±0.000
Zn	0.153±0.044	0.125±0.073	0.076±0.037	0.079±0.165	0.045±0.073	0.071±0.058	0.068±0.009
Ba	0.129±0.046	0.111±0.024	0.079±0.028	NR	NR	0.033±0.027	0.042±0.005
Sb	0.020±0.010	0.010±0.005	0.008±0.007	NR	NR	0.007±0.006	0.001±0.000
Sn	0.025±0.014	0.011±0.008	0.010±0.010	NR	NR	0.005±0.004	0.001±0.000
Co	0.001±0.000	0.001±0.000	0.001±0.000	0.009±0.015	0.013±0.029	NR	NR
Cd	0.000±0.000	0.000±0.000	0.000±0.000	0.000±0.000	0.000±0.000	NR	NR

The contributions of water-soluble ions were more abundant in the commercial area (3.81±1.08%), followed by Rf (3.28±0.16%), the residential area (1.51±0.54%) and the industrial sector (1.39±0.26%). These percentages were similar to those obtained for road dust from the center of Barcelona (~ 2.41%) but were higher than those reported in ring roads and for construction dust in the same city (Table 4). The results were also lower than those reported in cities in northern China influenced by coal combustion (4–7%, Zhao et al., 2006), and were higher than findings for road dust from the main streets in Fushun, where the contribution of water–soluble compounds was < 0.5% (Table 4). The ions with the highest contributions were Br^- (0.43–1.61%), SO_4^{2-} (up to 1.55%) and NH_4^+ (0.12–1.15%).

The largest contribution of trace elements was registered in the samples from the commercial sectors (0.53±0.15%), followed by the industrial areas (0.46±0.22%), residential zones (0.41±0.19%) and Rf (0.25±0.01%). These results show that the selection of the reference point was appropriate as it registered the lowest pollution with anthropogenic trace elements, thus allowing it to be considered an urban background site. The percentage of trace elements contribution from the commercial sectors was similar to that obtained in a Chinese city famed for coal production (Fushun) (~ 0.66%), and higher than that registered in the city center (~ 0.36%) and ring roads in Barcelona (~ 0.26%), affected mainly by road traffic (Table 4). The elements that registered the highest contributions were Zn (up to 0.17%) and Cu (up to 0.05%).

The highest OC contributions were obtained in Rf (29.04±1.45%), which could be associated with biogenic organic carbon. The commercial, industrial and residential zones registered OC values of

19.4±7.1%, 14.3±6.9% and 12.7±5.8%, respectively. These percentages were higher than those recorded in road dust, roadside dust and building dust in Barcelona, Birmingham, New Delhi and Fushun (Table 4), which could be associated with the predominance of gasoline vehicles in Bogota (~ 95%). However, the percentages obtained were in the range reported for road dust in commercial and residential areas of South Korean (Han et al., 2011) and Chinese cities (Zhao et al., 2006). On the other hand, the highest EC contribution was obtained in the commercial areas (1.94±0.70%), where diesel trucks predominated, with a similar percentage to the one reported for road dust in Barcelona. This was higher than that found in Birmingham and New Delhi, but lower than that obtained in Fushun (Table 4), where the use of coal is common.

The unaccounted mass in these profiles was 34% in the industrial dust, 29% in the residential dust, 13% in the commercial dust and 12% at the Rf point. The average unaccounted mass across all four sectors was 22%. This percentage includes components not measured in the samples (organic compounds and absorbed moisture, for example) and the oxygen present in the oxides of Si, Al, Fe, Ba, among others.

3.3. Spatial variability

CoD values ranged from 0.15 to 0.43 in commercial areas (Supplementary Table 3). The majority of combinations registered values < 0.30 suggesting a moderate similarity between the samples. C1 vs C3 (0.43), and C1 vs C4 (0.42) were the only two combinations exhibiting CoD values higher than 0.40. This indicates a moderate heterogeneity in chemical composition among points located in the north (C1), center (C4) and south (C3) of Bogota. The CoD values ranged from 0.17 to 0.56 in the industrial zones. The highest level of similarity (0.17) was obtained at the points I2 and I5, located in the same industrial area (Puente Aranda) in the geographical center of the city. The chemical profiles of samples I1 and I3 showed a moderate heterogeneity (0.56), suggesting that the chemical composition may vary from one industrial zone to another. Meanwhile, in the residential areas, the CoD values ranged from 0.19 to 0.61. All the combinations showed a moderate similarity (CoD < 0.30), although R2 registered values > 0.40 with the other profiles, indicating a moderate level of heterogeneity. The R2 and R3 combination (CoD = 0.61) stood out, indicating a low degree of similarity between samples from the north-west and north-east of the city.

After evaluating the level of divergence between the zones studied (considering the averages of the individual chemical profiles), it was found that the Rf composition was moderately heterogeneous with respect to the residential (0.64) and industrial areas (0.58) (Supplementary Table 4). The composition of the industrial and residential road dust registered a high degree of similarity (0.18).

3.4. Source identification

3.4.1. Variability of concentration levels

Samples from residential sectors showed high concentrations of Ca, As, Sr, V, Li, Rb and Co (Tables 2 and 3). These elements have been registered in areas influenced by fugitive dust from demolition and construction activities (Amato et al., 2009b; Crilley et al., 2017). This suggests that the residential dust was enriched with emissions from construction works. The prominent presence of Ca and trace elements (such as V, Co, Rb and As) may also be indicative of pavement erosion (Arditsoglou and Samara, 2005; Fullová et al., 2017), the poor state of the pavement (Amato et al., 2014b) and the contribution of soils. The point located furthest south in the city (R5) stood out for its high contributions of Ca (25%) and Sr (0.2%) to PM_{10} mass. These percentages were up to four times higher than those of the other samples, indicating enrichment of the road dust with fugitive emissions from the cement industry and quarries located south of the city.

The industrial samples presented average concentrations of the majority of components, but they registered high values of Pb, Ni and Zn (Table 3). Pollution from these elements could be associated with the deposition of particles emitted by industrial sources at high temperatures, such as metallurgical works and the burning of fossil fuels (Nicholson and Branson, 1993; Jeon et al., 2017; Ramírez et al., 2018a). Other stationary sources could be the fertilizer industry (Gabarrón et al., 2017) and solvent-based paint factories (Colnodo et al., 2016). Concentrations of Pb, Ni and Zn could also indicate contributions of non-exhaust emissions from road traffic, especially from wear of brake linings and tire tread (Thorpe and Harrison, 2008). I4 stood out for registering high contributions of Zn (0.74%) to PM_{10} mass, which was up to three times higher than the values from other industrial sites. Considering that I4 was located on an avenue with high vehicular congestion predominated by a "stop and go" pattern, Zn could be associated with tire rubber wear (Apeagyei et al., 2011; Amato et al., 2013). The characterization of I4 in terms of type of traffic (heavy) and road class (major road) could influence the high contributions of Zn to road dust (Apeagyei et al., 2011). Although gasoline lead was eliminated in Colombia in 1991, Pb can persist for several decades in soil/dust due to previous vehicle exhaust emissions (Shen et al., 2016).

Road dust from the commercial sector registered significant concentrations of EC, Al, Si, K, Mg, Na and S (Tables 2 and 3). The EC levels suggest that the samples were enriched by exhaust emissions from road traffic, particularly from diesel vehicles (trucks, buses and vans without emission control systems), as previous studies have reported that diesel engines emit more EC than gasoline ones (Ntziachristos et al., 2007; Robert et al., 2007). The high correlation between EC, OC and S ($r > 0.85$) reinforces this idea, since these species are tracer particles for combustion sources. The enrichment of

the samples by secondary compounds, particularly SO_4^{2-}, suggests the influence of combustion sources due to the presence of precursor gases such as SO_2 (Wang–Li, 2015). This is evidenced by observing the high correlation between OC, EC and SO_4^{2-} ($0.84 < r < 0.98$). Concentrations of minerals and trace metals, such as Cu, Ba, Sb and Cr, have been associated with non-exhaust emissions (Pant and Harrison, 2013). Trace elements such as Cu, Ba, Sb, Cr, Zr, Sn, Ni and Cd imply the enrichment of dust with metals emitted by brake and tire wear (Garg et al., 2000; Wahlin et al., 2006; Tanner et al., 2008; Sjödin et al., 2010; Duong and Lee, 2011). However, as has been shown in other research, it is not easy to distinguish between wear and tear emissions and crustal dust because their chemical composition is very similar (Bukowiecki et al., 2010). The samples located in the center of the city (C6 and C7) recorded the highest contributions of EC to PM_{10} mass (2.5% and 2.7%, respectively), which is explained by their being collected near diesel bus stops.

Finally, dust from Rf exhibited the highest percentages of OC and Fe, which have been identified as important soil constituents (Chow et al., 2003). Previous studies have reported that urban parks include a large proportion of green space, which can store considerable amounts of soil organic carbon (Strohbach et al., 2012). High values of OC could also indicate contamination by pesticides, fertilizers and wood preservatives (Nezat et al., 2017). As documented by previous researches in Bogota, OC concentrations can be explained not only by primary OC, but also by significant levels of secondary OC (Ramírez et al., 2018b). Although chlorine is the most abundant halogen in the atmosphere (Nilsson et al., 2013), the enrichment of this sample with chloride and ammonium (Table 2) could result from the deposition of secondary particles formed from precursor industrial gases such as HCl and NH_3 (Kelly et al., 2016). The presence of Cl^-, NH_4^+ and Br^- could also suggest soil enrichment by secondary particles from burning biomass (Nilsson et al., 2013; Phan et al., 2013).

3.4.2. Enrichment Factors (EFs)

In order to identify the anthropogenic influence of twelve selected elements, EFs were calculated based on concentrations of an urban background sample (Rf), using Al as the reference element (Fig. 4). Ba, Ca, Cd, Cr, Cu, Ni, Pb, Sb, Sn, Sr, V and Zn were selected because they have been identified as characteristic pollutants of road dust (Schauer et al., 2006; Thorpe and Harrison, 2008; Wei and Yang, 2010).

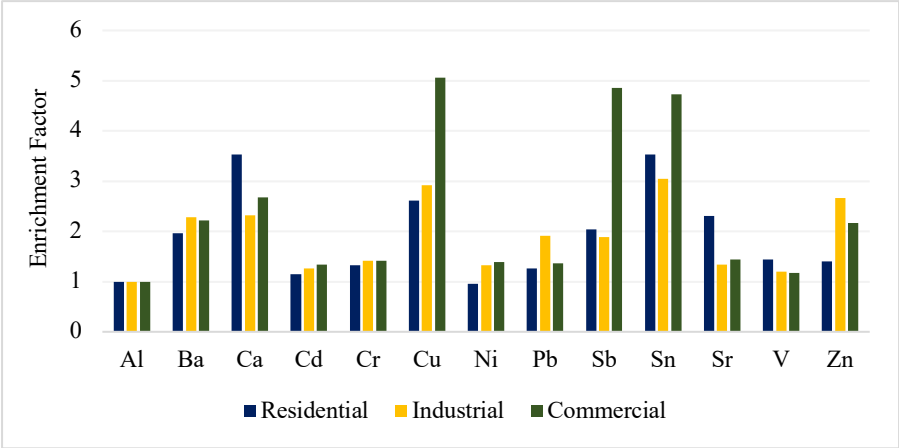

Fig. 4. Enrichment factors for road dust samples from residential, industrial and commercial areas.

All elements recorded values higher than 1 for the three urban areas, indicating a dominant antropogenic influence. Cadmium, Cr, Ni, Pb and V registered a minimum enrichment in all zones (EF < 2), which could be associated with pavement wear and industrial emissions. A moderate enrichment (EF = 2–5) of Ca–Cu–Sb–Sn and Sr was registered in the residential and commercial areas. These elements could be related to non-exhaust emissions. The high correlation between Cu–Sb–Sn ($0.84 < r < 0.94$) suggests a common origin, possibly related to brake wear (Grigoratos and Martini, 2015). Ca and Sr did not have a significant correlation with other elements, but they did have a high correlation with each other ($r = 0.88$), indicating a different source, possibly associated with dust from construction activities.

A moderate enrichment of Ba–Ca–Cu–Sn and Zn was registered in both the industrial and commercial zones. A high correlation between Cu and Ba ($r > 0.91$) was notable in the industrial zone, which could indicate a high enrichment of the samples by brake wear emissions (Iijima et al., 2007). Other elements used as tracers for brake wear (Sb, Sn and Cu) also had a significant correlation with Cu and Ba ($r > 0.64$). Zn was correlated with Sb ($r > 0.75$) and to a lesser extent with Cu, Sn and Ba ($0.33 < r > 0.38$), indicating that Zn could come from another source such as tire wear. Calcium showed a significant correlation with Cu ($r = 0.71$) and a moderate correlation with Ba, Sb and Sn ($0.37 < r > 0.53$), suggesting that Ca could come from other sources, such as construction dust, crustal dust and asphalt wear (Fullová et al., 2017).

A significant enrichment of Cu was registered in the commercial zones, as well as significant levels of Sb and Sn, which have been associated with brake wear emissions (Duong and Lee, 2011). Cu and Zn displayed a strong correlation with each other ($r = 0.80$), and a moderate association with OC and EC, which could indicate soil contamination from lubricating oil (Cui et al., 2017). Tracers of non-exhaust emissions showed a moderate correlation with crustal elements, suggesting the presence of soil dust related to the poor state of roads. The high correlation of Zn with OC/EC ($r > 0.65$) was notable,

which could indicate an enrichment of road dust by exhaust emissions from diesel vehicles (Cui et al., 2017). This is supported by the significant correlation between Ba and OC/EC ($0.57 < r > 0.73$), as these elements have been used as tracers of diesel combustion (Peltier et al., 2011). The correlation between Zn and OC/EC could also indicate enrichment of road dust by tire wear emissions (Aatmeeyata and Sharma, 2010). Broadly speaking, no element recorded very high or extremely high enrichment levels, which could indicate that the selected background sample (urban park soil) was affected by urban emissions.

3.4.3. Ratios of specific elements

Specific element ratios can help identify emitting sources (Pant et al., 2015). As mentioned above, this study considered Al as the marker of soil dust, and hence the ratios of selected crustal elements (Fe, K, Ca, and Ti) to Al were calculated (Table 5).

K/Al and Ti/Al ratios showed insignificant variations in the areas studied, indicating a crustal influence in all road dust samples. A similar pattern has been observed in cities such as Barcelona and Xi'an (Table 5). The Fe/Al ratio in Rf was 1.8 times higher than the value for the residential sector, which can be explained by a high prevalence of biogenic iron oxides at the reference point. The enrichment of residential road dust by construction emissions was further supported by the Ca/Al ratio, which registered a value 3.5 times higher than at Rf. This is consistent with several studies that have reported higher values of Ca/Al ratio in construction and cement dust (Table 5). The point R5 stood out for registering a Ca/Al ratio of 4.21, the highest among all samples. This suggests that the road dust collected south of the city was highly enriched by fugitive emissions from cement industries and quarries.

Table 5. Comparison of elemental, carbonaceous and trace ratios in the thoracic fraction of road dust. NR: not reported.

	This study				Amato et al., 2009			Kong et al., 2011			Zhang et al., 2014		Pant et al., 2015	
	Bogota				**Barcelona**			**Fushun**			**Xi'an**		**Birmingham**	**New Delhi**
	Residential	Industrial	Commercial	Reference site (urban park)	City center	Ring roads	Construction	Road dust	Construction	Cement	Road dust	Cement	Roadside	Roadside
Fe/Al	0.41	0.49	0.54	0.75	1.21	0.94	0.89	0.15	0.12	0.26	0.55	0.55	0.85	0.78
K/Al	0.11	0.14	0.15	0.11	0.33	0.36	0.35	0.03	0.05	0.20	0.29	0.22	NR	NR
Ca/Al	0.95	0.63	0.72	0.27	3.05	2.73	3.60	1.29	4.04	6.30	1.75	3.89	0.37	1.26
Ti/Al	0.06	0.06	0.06	0.06	0.07	0.07	0.07	0.06	0.07	0.12	0.06	0.05	<0.01	0.01
Cu/Sb	10.2	12.3	8.29	7.94	6.96	7.56	6.46	NR	NR	NR	NR	NR	5.0	16.0
Zn/Sb	40.6	83.6	26.3	59.2	7.66	12.3	9.93	NR	NR	NR	NR	NR	10.1	68
OC/TC	0.96	0.98	0.91	0.97	0.80	0.84	0.88	0.57	0.54	0.49	NR	NR	0.98	0.78
OC/EC	24.1	57.9	9.95	38.2	4.10	5.39	7.31	1.30	1.19	0.99	NR	NR	60.8	3.57

The Cu/Sb ratio has been used as an indicator of brake wear (Han et al., 2011; Amato et al., 2013). Cu/Sb is approximately 125 in soil dust (Thorpe and Harrison, 2008) and 70 in continental crust (Rudnick and Gao, 2003). Hence, lower Cu/Sb values could suggest higher contributions of brake wear dust. In our case, the average ratio was 11±3 across all samples, which coincided with the value for non-asbestos organic brake pads (Iijima et al., 2007). This is indicative of an enrichment of road dust by brake wear. The value obtained was higher than that reported in Barcelona and Birmingham, but it was lower than data from New Delhi (Table 5). Cu/Sb values from 8.3 to 12.3 were obtained, indicating that commercial road dust recorded higher contributions of brake wear (8.3) than the residential (10.2) and industrial samples (12.3).

The Zn/Sb ratio can be used to differentiate contributions of tire and brake wear emissions. Zn was chosen because it is a tracer element for tire emission (Schauer et al., 2006; Gustafsson et al., 2008), some studies even reportinng that Zn concentrations in tires are about 15 times higher than in brakes (Apeagyei et al., 2011). Sb was selected because it has been associated with brake wear (Gietl et al., 2010; Amato et al., 2013; Quiroz et al., 2013). The average ratio across all samples was 53±28, which emphasizes that the road dust samples were highly enriched by tire wear. This value is much higher than that registered in Barcelona and similar to that reported in New Delhi (Table 5). Samples from the industrial sector registered a Zn/Sb ratio of 84, twice the average of the residential sector (41) and three times higher than that of the commercial sector (26). The point I4, located on a road with heavy traffic, was notable for its Zn/Sb ratio of 125. These results are consistent with the enrichment factors analysis and are in agreement with previous studies that have reported high concentrations of Zn in road dust impacted by heavy traffic (Apeagyei et al., 2011). Other potential industrial sources of Zn are related to galvanizing activities and rubber production (Zhao et al., 2006).

The OC/TC ratios ranged between 0.91 and 0.98, showing that TC was mainly in the form of OC. The linear correlation between OC and TC (r = 0.99) across all samples confirms this idea. These values were higher than those reported in Barcelona, Fushun and New Delhi, but were similar to those found in Birmingham (Table 5). This can be explained by the main type of vehicle used in Bogota, which uses gasoline (~ 95%) and emits predominantly OC (Schauer et al., 2006). The higher concentrations of EC (Table 2) associated with exhaust emissions from diesel vehicles could explain the low OC/EC ratio in the commercial zone.

3.4.4. Particle morphology

SEM images provide additional information about grain size and shape of individual road dust particles (Mummullage et al., 2016). Spherical particles of Pb (~ 2 μm) were noted in the Rf site, indicating an accumulation of this element in urban park soil due to industrial combustion and

previous vehicle exhaust emissions (Fig. 5a). Spherical particles of Fe < 5 μm were also observed in Rf (Fig. 5b), which suggests an accumulation of emissions from motor vehicle and high-temperature industrial processes. This confirms that the Rf site was affected by urban emissions. Spherical and semispherical particles of Fe, Cu and Pb < 10 μm were also found in the commercial, industrial and residential samples (Figs. 5c and 5d). Particles of Ba, Zn, Cu, Fe, Mn, Sn and Pb with an angular and subangular shape (Fig. 5e–5h) indicate an enrichment of road dust with particles ranging between 2 μm and 10 μm from vehicle and pavement wear.

3.4.5. Principal component analysis

A Principal Component Analysis (PCA) was conducted in order to identify the factors that could explain the variance of tracer chemical species in the PM_{10} fraction. PCA methods have been widely used to identify pollution sources of road dust in geochemical studies (Amato et al., 2009b; Wang et al., 2012; Pan et al., 2017). A Varimax rotation was applied to facilitate the interpretation of the results. Elements with communality > 0.7 were considered and factors whose eigenvalues were > 1 were retained. Five factors were identified, accounting for 91% of the total variance of the whole dataset (Table 6).

The principle component (PC1) explains 63% of the total variance and is dominated by V, Al, Rb, As, Fe, K, Co, Ti, Cr, Mg, Cd, Ni, P, Ba and OC. According to the analyses presented in the previous paragraphs, this factor is related to natural and anthropogenic sources, and is representative of local soils, pavement erosion and the poor condition of the pavement.

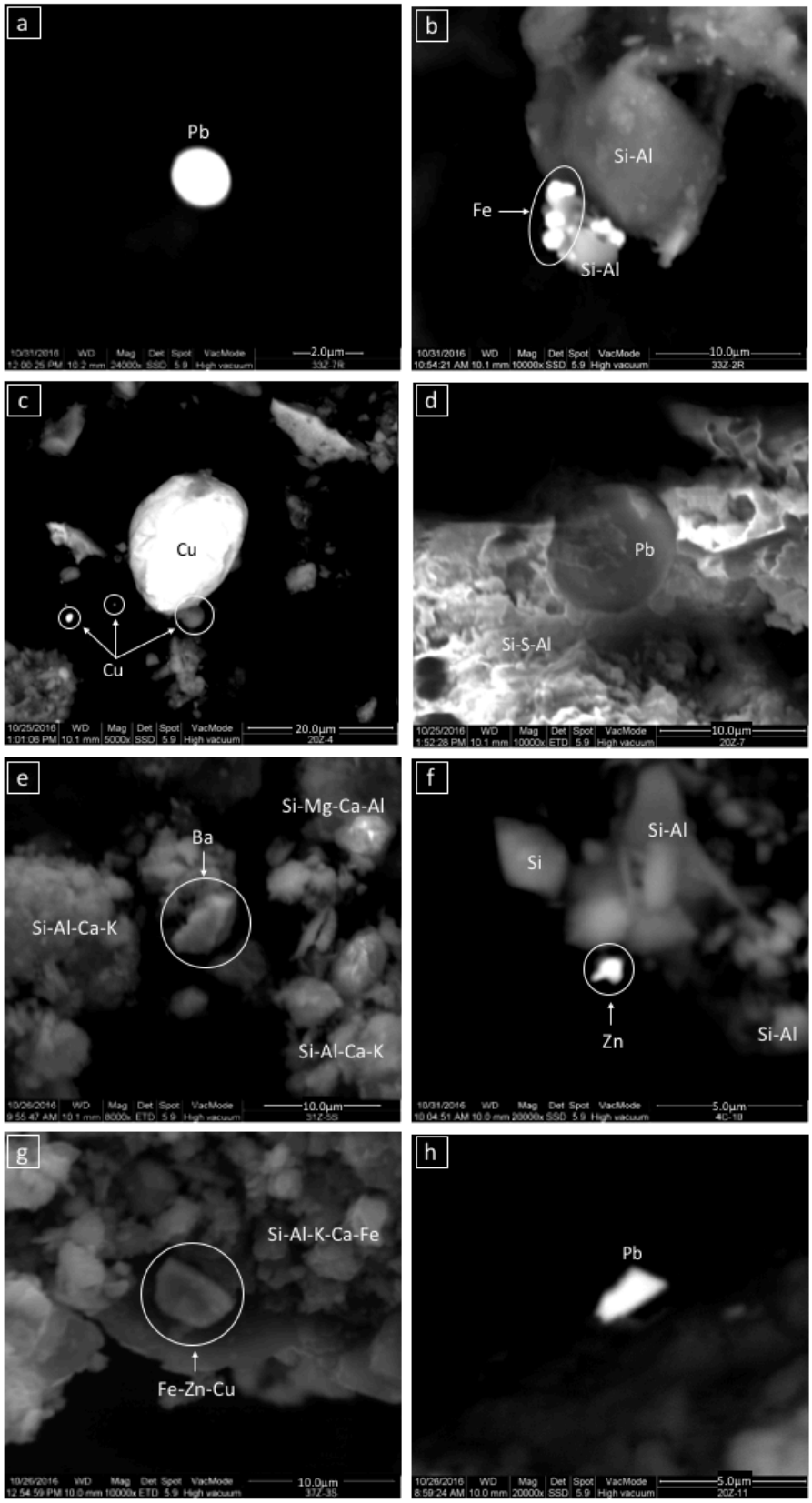

Fig. 5. SEM images of road dust in Bogota. (a)(b) spherical particles of Pb and Fe in the urban background site; (c)(d) spherical and semispherical particles of Cu and Pb in a residential road dust sample; (e)(f)(g)(h) particles of Ba, Zn, Cu and Pb with angulated and subangulated morphology from vehicular and pavement wear.

562 Table 6. Rotated component of PCA for road dust in Bogota (n = 20). Only significant values (> 0.32, according
563 to Yongming et al., 2006) are shown. Highest values are highlighted in bold.

Element	PC1	PC2	PC3	PC4	PC5	Communality
V	**0.95**					0.98
Al	**0.93**					0.96
Rb	**0.93**					0.97
As	**0.92**	0.36				0.97
Fe	**0.91**	0.32				0.98
K	**0.86**	0.39				0.91
Co	**0.85**		0.35			0.97
Ti	**0.84**	0.50				0.99
Cr	**0.83**		0.41			0.77
Mg	**0.78**	0.58				0.89
Cd	**0.76**		0.51			0.97
Ni	**0.76**		0.40			0.97
P	**0.74**	0.35	0.46			0.93
Ba	**0.71**		0.50	0.35		0.81
OC	**0.49**		0.46		0.46	0.88
S		**0.93**				0.84
Ca	0.39	**0.89**				0.98
Sr	0.48	**0.85**				0.99
Zn			**0.85**			0.97
Pb	0.43		**0.82**			0.87
Na	0.33	0.50	**0.66**			0.80
Sb				**0.89**		0.84
Cu	0.40		0.42	**0.73**		0.88
Sn	0.44		0.36	**0.57**	0.38	0.81
EC				0.35	**0.84**	0.91
Eigenvalue	15.7	3.21	1.57	1.35	1.01	
Variance (%)	62.8	12.8	6.29	5.40	4.02	
Cumulative variance (%)	62.8	75.6	81.9	87.3	91.3	

564

565 PC2 explains 13% of the total variance and has high loadings for S, Ca and Sr. This factor mainly
566 represents dust from construction and demolition activities, enriched with soil dust. PC3 explain 6% of
567 the total variance. The significant presence of Zn, Pb and Na suggests an industrial origin. Moderate
568 values of OC, Cr, Co, Cd, Ni and Cu are consistent with that denomination. PC4 explain 5% of the
569 total variance and is related to tracers of non-exhaust emissions. High loading of Sb, Cu and Sn is
570 representative of brake wear. This denomination is consistent with the presence of Ba. Enrichment of
571 these elements by wear of other metal parts of vehicles and industrial emissions is not ruled out.
572 Finally, PC5 explains 4% of the total variance and has high loadings for EC and moderate presence of
573 OC, representing tailpipe emissions from road traffic, particularly from diesel vehicles.

574

575 **4. Conclusions**

576

577 Previous studies have reported that 23% of the airborne PM_{10} mass is contributed by road dust
578 resuspension in Bogota (Ramírez et al., 2018a). The present study has explored this topic further by
579 analyzing the inorganic chemical composition and identifying possible sources of the thoracic fraction
580 in road dust from representative industrial, residential and commercial areas in Bogota. Size
581 distribution revealed that the volume (%) of the PM_{10} fraction was higher in industrial road dust

samples (9.9%) than in the residential (8.7%) and commercial (7.8%) ones. The most abundant major components were Si (26.7±15.5%), OC (14.7±7.8%) and Al (10.1±5.9%). SO_4^{2-} (0.9±0.4%) and NH_4^+ (0.2±0.1%) were the most prevalent water-soluble ions. Ti, Ba and Zn were the most abundant trace elements, followed by Mn, Sr, Cu, Pb and Zr. The results showed that crustal elements accounted for 49–62% of the PM_{10} mass, followed by OC (13–29%), water-soluble ions (1.4–3.8%), EC (0.8–1.9%) and trace elements (0.2–0.5%). CoD indicated that the chemical profiles of the PM_{10} fraction from industrial and residential road dust registered a high similarity (0.18).

The chemical composition of the residential road dust revealed an enrichment by emissions from construction works and road pavement erosion. The industrial samples contained significant concentrations of Pb and Zn, possibly originating from industrial sources at high temperatures. Road dust from the commercial sector registered enrichement by exhaust emissions, particularly from diesel vehicles, and trace metals from non-exhaust emissions. The reference sample (urban park soil) registered significant concentrations of OC and Fe, which could have a natural origin. The enrichment factors revealed that Cd-Cr-Ni-Pb-V could be associated with pavement wear and industrial emissions, Cu-Sb-Sn with non-exhaust emissions and Ca-Sr with construction dust. The ratios analysis suggested an enrichment of residential road dust by construction and cement dust. It also indicated enrichment of road dust by brake wear and tire wear, especially in commercial and industrial zones, respectively. The five components obtained by PCA (local soils and pavement erosion, construction and demolition activities, industrial emissions, brake wear and tailpipe emissions) accounted for 91% of the total variance in the whole dataset. The morphological analysis enabled the identification of spherical particles of Pb, Cu and Fe, and subangular particles of Ba, Zn, Cu, Fe, Mn, Sn and Pb with sizes < 10 μm.

The results provide data for a better understanding of road dust in Bogota, one of the main sources of PM_{10} emissions in the city, . These data will be useful to optimize environmental and health policies by preventive and corrective measures such as paving roads, repairing pavements in poor condition, covering truck loads and construction material, relocating industrial activities and implementing efficient sweeping and street washing programs.

Acknowledgments

The authors would like to thank the Universidad Internacional de Andalucía (UNIA) and the Regional Council for the Environment of the Junta de Andalucía for partially funding this project. We also thank Diana Ramírez (Monash University) for her comments.

Appendix A. Supplementary data

Supplementary data to this article can be found online at

References

Aatmeeyata, Sharma, M., 2010. Polycyclic aromatic hydrocarbons, elemental and organic carbon emissions from tire–wear. Sci. Total Environ. 408, 4563–4568.

Amato, F., Cassee, F., van der Gon, H., Gehrig, R., Gustafsson, M., Hafner, W., Harrison, R., Jozwicka, M., Kelly, F., Moreno, T., Prevot, A., Schaap, M., Sunyer, J., Querol, X., 2014a. Urban air quality: The challenge of traffic non–exhaust emissions. J. Hazard. Mater. 275, 31–36.

Amato, F., Alastuey, A., de la Rosa, J., Gonzalez, Y., Sánchez de la Campa, A. M., Pandolfi, M., Lozano, A., Contreras, J., Querol, X., 2014b. Trends of road dust emissions contributions on ambient air particulate levels at rural, urban and industrial sites in southern Spain. Atmos. Chem. Phys., 14, 3533–3544.

Amato, F., Schaap, M., Denier van der Gon, H., Pandolfi, M., Alastuey, A., Keuken, M., Querol, X., 2013. Short–term variability of mineral dust, metals and carbon emission from road dust resuspension. Atmos. Environ. 74, 134–140.

Amato, F., Querol, X., Alastuey, A., Pandolfi, M., Moreno, T., Gracia, J., Rodriguez, P., 2009a. Evaluating urban PM_{10} pollution benefit induced by street cleaning activities. Atmos. Environ. 43, 4472–4480.

Amato, F., Pandolfi, M., Viana, M., Querol, X., Alastuey, A., Moreno, T., 2009b. Spatial and chemical patterns of PM_{10} in road dust deposited in urban environment. Atmos. Environ. 43, 1650–1659.

Apeagyei, E., Bank, M., Spengler, J., 2011. Distribution of heavy metals in road dust along an urban–rural gradient in Massachusetts. Atmos. Environ 45, 2310–2323.

Arditsoglou, A., Samara, C., 2005. Levels of total suspended particulate matter and major trace elements in Kosovo: a source identification and apportionment study. Chemosphere 59, 669–678.

Beltran, D., Belalcazar, L., Rojas, N., 2012. Spatial distribution of non–exhaust particulate matter emissions from road traffic for the city of Bogota – Colombia. 2012 International Emission Inventory Conference "Emission Inventories – meeting the challenges posed by emerging global, national, regional and local air quality issues". https://www3.epa.gov/ttn/chief/conference/ei20/index.html, (accessed 07 april 2018).

Birch, M., Cary, R., 1996. Elemental carbon–based method for monitoring occupational exposures to particulate diesel exhaust. Aerosol Sci. Technol. 25(3), 221–241.

Birmili, W., Allen, A.G., Bary, F., Harrison, R.M., 2006. Trace metal concentrations and water solubility in size–fractionated atmospheric particles and influence of road traffic. Environ. Sci.

Technol. 40, 1144–1153.

Bukowiecki, N., Lienemann, P., Hill, M., Furger, M., Richard, A., Amato, F., Prevot, A.S.H., Baltensperger, U., Buchmann, B., Gehrig, R., 2010. PM_{10} emission factors for non–exhaust particles generated by road traffic in an urban street canyon and along a freeway in Switzerland. Atmos. Environ. 44 (19), 2330–2340.

Burnett, R., Pope, A., Ezzati, M., Olives, C., Lim, S., Mehta, S., Shin, H., Singh, G., Hubbell, B., Brauer, M., Anderson, H., Smith, K., Balmes, J., Bruce, N., Kan, H., Laden, F., Prüss–Ustün, A., Turner, M., Gapstur, S., Diver, W., Cohen, A., 2014. An intgrated risk function for estimating the global burden of disease attributable to ambient fine particulate matter exposure. Environ. Health Perspect. 122(4), 307–404.

Calvo, A., Alves, C., Castro, A., Pont, V., Vicente, A., Fraile, R., 2013. Research on aerosol sources and chemical composition: Past, current and emerging issues. Atmos. Res. 120–121, 1–28.

Cavalli, F., Viana, M., Yttri, K.E., Genberg, J., Putaud, J., 2010. Toward a standardised thermal–optical protocol for measuring atmospheric organic and elemental carbon: the EUSAAR protocol. Atmos. Meas. Tech. 3, 79–89.

CCA – Cámara de Comercio de Bogotá, 2017. Observatorio de movilidad. Universidad de Los Andes/CCA, Bogotá.

CEPAL – Comisión Económica para América Latina y el Caribe, 2005. Latin America: urban and rural population projections. United Nations, Chile.

Chen, H., Kwong, J., Copes, R., Hystad, P., van Donkelaar, A., Tu, K., Brook, J., Goldberg, M., Martin, R., Murray, B., Wilton, A., Kopp, A., Burnett, R., 2017. Exposure to ambient air pollution and the incidence of dementia: A population–based cohort study. Environ. Int. 108, 271–277.

Chow, J., Watson, J., Ashbaugh, L., Magliano, K., 2003. Similarities and differences in PM_{10} chemical source profiles for geological dust from the San Joaquin Valley, California. Atmos. Environ. 37, 1317–1340.

Cifuentes, L., Krupnick, A., O'Ryan, R., Toman, M., 2005. Urban air quality and human health in Latin America and The Caribbean. PAHO, Washington D.C.

Colnodo, RDS, IPEN, 2016. Plomo en pinturas a base de solventes para uso doméstico en Colombia. Colnodo/Red de Desarrollo Sostenible, Bogotá.

Crilley, L., Lucarelli, F., Bloss, W., Harrison, R., Beddows, D., Calzolai, G., Nava, S., Valli, G., Bernardoni, V., Vecchi, R., 2017. Source apportionment of fine and coarse particles at a roadside and urban background site in London during the 2012 summer ClearfLo campaign. Environ. Pollut 220, 766–778.

Cui, M., Chen, Y., Feng, Y., Li, Ch., Zheng, J., Tian, Ch., Yan, C., Zheng, M., 2017. Measurement of PM and its chemical composition in real–world emissions from non–road and on–road diesel vehicles. Atmos. Chem. Phys. 17, 6779–6795.

DANE – Departamento Administrativo Nacional de Estadística, 2010. Proyecciones nacionales y departamentales de población 2005–2020. DANE, Bogotá.

Demographia, 2018. Demographia World Urban Areas. 14th annual edition. http://demographia.com/db–worldua.pdf (accessed 07 April 2018).

Du, Y., Xu, X., Chu, M., Guo, Y., Wang, J., 2016. Air particulate matter and cardiovascular disease: the epidemiological, biomedical and clinical evidence. J. Thorac. Dis. 8(1), E8–E19. doi: 10.3978/j.issn.2072–1439.2015.11.37.

Duong, T., Lee, B., 2011. Determining contamination level of heavy metals in road dust from busy traffic areas with different characteristics. J. Environ. Manage. 92(3), 554–562.

Fujiwara, F., Gomez, D., Dawidowski, L., Perelman, P., Faggi, A., 2011b. Metals associated with airborne particulate matter in road dust and tree bark collected in a megacity (Buenos Aires, Argentina). Ecol. Indic. 11(2), 240–247.

Fujiwara, F., Jiménez, R., Dawidowski, L., Gómez, D., Polla, G., Pereyra, V., Smichowski, P., 2011a. Spatial and chemical patterns of size fractionated road dust collected in a megacitiy. Atmos. Environ. 45, 1497–1505.

Fullová, D., Durcanska, D., Hegrová, J., 2017. Impact of asphalt mixture composition on particulate matter production. Procedia Eng. 192, 201–206.

Gabarrón, M., Faz, A., Acosta, J., 2017. Effect of different industrial activities on heavy metal concentrations and chemical distribution in topsoil and road dust. Environ. Earth Sci. 76:129. doi: 10.1007/s12665–017–6449–4.

Garg, B., Cadle, S., Mulawa, P., Groblicki, P., 2000. Brake wear particulate matter emissions. Environ. Sci. Technol. 34, 4463–4469.

Gent, J., Koutrakis, P., Belanger, K., Triche, E., Holford, T., Bracken, M., Leaderer, B., 2009. Symptoms and medication use in children with asthma and traffic–related sources of fine particle pollution. Environ. Health. Perspect. 117(7), 1168–1174.

Gietl, J., Lawrence, R., Thorpe, A., Harrison, R., 2010. Identification of brake wear particles and derivation of a quantitative tracer for brake dust at a major road. Atmos. Environ. 44(2), 141–146.

Green, J., Sánchez, S., 2013. Air quality in Latin America: an overview. Clean Air Institute, Washington D.C.

Grigoratos, T., Martini, G., 2015. Brake wear particle emissions: a review. Environ. Sci. Pollut. Res. 22, 2491–2504.

Grobéty, B., Gieré, R., Dietze, V., Stille, P., 2010. Airborne particles in the urban environment. Elements 6(4), 229–234.

761 Gulia, S., Nagendra, S., Khare, M., Khanna, I., 2015. Urban air quality management – A review.
762 Atmos. Pollut. Res. 6, 286–304.
763
764 Gunawardana, Ch., Goonetilleke, A., Egodawatta, P., Dawes, L., Kokot, S., 2012. Source
765 characterisation of road dust based on chemical and mineralogical composition. Chemosphere 87,
766 163–170.
767
768 Gurjar, B., Jain, A., Sharma, A., Agarwal, A., Gupta, P., Nagpure, A., Lelieveld, J., 2010. Human
769 health risks in megacities due to air pollution. Atmos. Environ. 44, 4606–4613.
770
771 Gustafsson, M., Blomqvist, G., Gudmundsson, A., Dahl, A., Swietlicki, E., Bohgard, M., Lindbom, J.,
772 Ljungman, A., 2008. Properties and toxicological effects of particles from the interaction between
773 tires, road pavement and winter traction material. Sci. Total Environ. 393, 226–40.
774
775 Ha, S., Hu, H., Roussos–Ross, D., Haidong, K., Roth, J., Xu, X., 2014. The effects of air pollution on
776 adverse birth outcomes. Environ. Res. 134, 198–204.
777
778 Han, S., Youn, J., Jung, Y., 2011. Characterization of PM_{10} and $PM_{2.5}$ source profiles for resuspended
779 road dust collected using mobile sampling methodology. Atmos. Environ. 45, 3343–3351.
780
781 Huang, L., Yuan, Ch., Wang, G., Wang, K., 2011. Chemical characteristics and source apportionment
782 of PM_{10} during a brown haze episode in Harbin, China. Particuology 9, 32–38.
783
784 IDEAM – Instituto de Hidrología, Meteorología y Estudios Ambientales, 2016. Informe del estado de
785 la calidad del aire en Colombia 2011 – 2015. IDEAM/MinAmbiente, Bogotá.
786
787 IDEAM, 2015a. Atlas climatológico de Colombia – Interactivo.
788 http://atlas.ideam.gov.co/visorAtlasClimatologico.html (accessed 09 November 2017).
789
790 IDEAM, 2015b. Atlas de vientos de Colombia – Interactivo.
791 http://atlas.ideam.gov.co/visorAtlasVientos.html (accessed 09 November 2017).
792
793 IHME – Institute for Health Metrics and Evaluation, 2017. State of global air. A special report on
794 global exposure to air pollution and its disease burden. Health Effects Institute, Boston.
795
796 Iijima, A., Sato, K., Yano, K., Tago, H., Kato, M., Kimura, H., Furuta, N., 2007. Particle size and
797 composition distribution analysis of automotive brake abrasion dusts for the evaluation of antimony
798 sources of airborne particulate matter. Atmos. Environ. 41, 4908–4919.
799
800 Int Panis, L., Provost, E., Cox, B., Louwies, T., Laeremans, M., Standaert, A., Dons, E., Holmstock,
801 L., Nawrot, T., De Boever, P., 2017. Short–term air pollution exposure decreases lung function: a
802 repeated measures study in healthy adults. Environ. Health 16:60. https://doi.org/10.1186/s12940–
803 017–0271–z.
804
805 Jeon, S., Kwon, M., Yang, J., Lee, S., 2017. Identifying the source of Zn in soils around a Zn smelter
806 using Pb isotope ratios and mineralogical analysis. Sci. Total. Environ. 601–602, 66–72.
807
808 Kelly, J., Baker, K., Nolte, C., Napelenok, S., Keene, W., Pszenny, A., 2016. Simulating the phase

809 partitioning of NH_3, HNO_3, and HCl with size–resolved particles over northern Colorado in winter.
810 Atmos. Environ. 131, 67–77.
811
812 Kioumourtzoglou, M., Schwartz, J., Weisskopf, M., Melly, S., Wang, Y., Dominici, F., Zanobetti, A.,
813 2016. Long–term $PM_{2.5}$ exposure and neurological hospital admissions in the Northeastern United
814 States. Environ. Health Perspect. 124, 23–29.
815
816 Kong, Sh., Ji, Y., Lu, B., Chen, L., Han, B., Li, Z., Bai, Z., 2011. Characterization of PM_{10} source
817 profiles for fugitive dust in Fushun–a city famous for coal. Atmos. Environ. 45, 5351–5365.
818
819 Kupiainen, K., Tervahattu, H., Räisänen, M., Mäkelä, T., Aurela, M., Hillamo, R., 2004. Size and
820 composition of airborne particles from pavement wear, tires, and traction sanding. Environ. Sci.
821 Technol. 39, 699–706.
822
823 Lee, J., Lee, S., Bae, G., 2014. A review of the association between air pollutant exposure and allergic
824 diseases in children. Atmos. Pollut. Res. 5, 616–629.
825
826 Ma, M., Li, Sh., Jin, H., Zhang, Y., Xu, J., Chen, D., Chen, K., Zhou, Y., Xiao, Ch., 2015.
827 Characteristics and oxidative stress on rats and traffic policemen of ambient fine particulate matter
828 from Shenyang. Sci. Total Environ. 526, 110–115.
829
830 Ma, X., Jia, H., 2016. Particulate matter and gaseous pollutions in three megacities over China:
831 Situation and implication. Atmos. Environ. 140, 476–494.
832
833 Men, C., Liu, R., Xu, F., Wang, Q., Guo, L., Shen, Z., 2018. Pollution characteristics, risk assessment,
834 and source apportionment of heavy metals in road dust in Beijing, China. Sci. Total. Environ. 612,
835 138–147.
836
837 Méndez, J., Pinto, L., Galvis, B., Pachón, J., 2017. Estimation of resuspended dust emission factors
838 before, during and after road paving process in Bogota. Cien. Ing. Neogranadina 27(1), 43–60.
839
840 Minguillón, M., Campos, A., Cárdenas, B., Blanco, S., Molina, L., Querol, X., 2014. Mass
841 concentration, composition and sources of fine and coarse particulate matter in Tijuana, Mexico,
842 during Cal–Mex campaign. Atmos. Environ. 88, 320–329.
843
844 Moosmüller, H., Gillies, J., Rogers, C., DuBois, D., Chow, J., Watson, J., Langston, R., 1998.
845 Particulate emission rates for unpaved shoulders along a paved road. J. Air Waste Manag. Assoc.
846 48(5), 398–407.
847
848 Moreno, T., Amato, F., Querol, X., Alastuey, A., Gibbons, W., 2008. Trace element fractionation
849 processes in resuspended mineral aerosols extracted from Australian continental surface materials.
850 Aust. J. Soil Res. 46, 128–140.
851
852 Moreno, T., Oldroyd, A., McDonald, I., Gibbons, W., 2007. Preferential fractionation of trace metals–
853 metalloids into PM_{10} resuspended from contaminated gold mine tailings at rodalquilar, Spain. Water
854 Air Soil Pollut. 179, 93–105.
855
856 Mummullage, S., Egodawatta, P., Ayoko, G., Goonetilleke, A., 2016. Use of physicochemical

857 signatures to assess the sources of metals in urban road dust. Sci. Total. Environ. 541, 1303–1309.
858
859 Nedbor–Gross, R., Henderson, B., Pérez–Peña, M., Pachón, J., 2018. Air quality modeling in Bogota,
860 Colombia using local emissions and natural mitigation factor adjustment for re–suspended particulate
861 matter. Atmos. Pollut. Res. 9(1), 95–104.
862
863 Nezat, C., Hatch, Sh., Uecker, T., 2017. Heavy metal content in urban residential and park soils: A
864 case study in Spokane, Washington, USA. Appl. Geochem. 78, 186–193.
865
866 Nicholson, K., Branson, J., 1993. Lead concentrations in U.K. urban air. Atmos. Environ. Part B.
867 Urban Atmosphere 27(2), 265–268.
868
869 Nilsson, E., Joelsson, L., Heimdal, J., Johnson, M., Nielsen, O., 2013. Re–evaluation of the reaction
870 rate coefficient of CH_3Br + OH with implications for the atmospheric budget of methyl bromide.
871 Atmos. Environ. 80, 70–74.
872
873 Ntziachristos, L., Ning, Z., Geller, M., Sheesley, R., Schauer, J., Sioutas, C., 2007. Fine, ultrafine and
874 nanoparticle trace element compositions near a major freeway with a high heavy–duty diesel fraction.
875 Atmos. Environ. 41, 5864–5866.
876
877 Pachón, J., Galvis, B., Lombana, O., Carmona, L., Fajardo, S., Rincón, A., Meneses, S., Chaparro, R.,
878 Nedbor–Gross, R., Henderson, B., 2018. Development and evaluation of a comprehensive
879 atmospheric emission inventory for air quality modeling in the megacity of Bogotá. Atmosphere 9(2),
880 49; https://doi.org/10.3390/atmos9020049.
881
882 Pacyna, J., 1998. Source inventories for atmospheric trace metals. In: Harrison, R., Van Grieken, R.
883 (Eds.). Atmospheric particles: IUPAC Series on Analytical and Physical Chemistry of Environmental
884 Systems, vol. 5. Wiley, pp. 387–423.
885
886 PAHO – Pan American Health Organization, 2005. An assessment of health effects of ambient air
887 pollution in Latin America and The Caribbean. PAHO, Washington, D.C.
888
889 Pan, H., Lu, X., Lei, K., 2017. A comprehensive analysis of heavy metals in urban road dust of Xi'an,
890 China: Contamination, source apportionment and spatial distribution. Sci. Total. Environ. 609, 1361–
891 1369.
892
893 Pant, P., Baker, S., Shukla, A., Maikawa, C., Pollitt, K., Harrison, R., 2015. The PM_{10} fraction of road
894 dust in the UK and India: Characterization, source profiles and oxidative potential. Sci. Total Environ.
895 530–531, 445–452.
896
897 Pant, P., Harrison, R. 2013. Estimation of the contribution of road traffic emissions to particulate
898 matter concentrations from field measurements: A review. Atmos. Environ. 77, 78–97.
899
900 Pearson, J., Bachireddy, C., Shyamprasad, S., Goldfine, A., Brownstein, J., 2010. Association
901 between fine particulate matter and diabetes prevalence in the U.S. Diabetes Care 33(10), 2196–2201.
902

Peltier, R., Cromar, K., Ma, Y., Fan, Z., Lippmann, M., 2011. Spatial and seasonal distribution of aerosol chemical components in New York City: (2) road dust and other tracers of traffic–generated air pollution. J. Expo. Sci. Environ. Epidemiol. 21(5), 484–494.

Perez, N., Pey, J., Cusack, M., Reche, C., Querol, X., Alastuey, A., Viana, M., 2010. Variability of particle number, black carbon, and PM_{10}, $PM_{2.5}$, and PM_1 levels and speciation: influence of road traffic emissions on urban air quality. Aerosol. Sci. Technol. 44, 487–499.

Phan, N., Kim, K., Shon, Z., Jeon, E., Jung, K., Kim, N., 2013. Analysis of ammonia variation in the urban atmosphere. Atmos. Environ. 65, 177–185.

Prada, D., Zhong, J., Colicino, E., Zanobetti, A., Schwartz, J., Dagincourt, N., Fang, Sh., Kloog, I., Zmuda, J., Holick, M., Herrera, L., Hou, L., Dominici, F., Bartali, B., Baccarelli, A., 2017. Association of air particulate pollution with bone loss over time and bone fracture risk: analysis of data from two independent studies. Lancet Planet Health. 1(8), e337–e347.

Prichard, H., Fisher, P., 2012. Identification of platinum and palladium particles emitted from vehicles and dispersed into the surface environment. Environ. Sci. Technol. 46, 3149–3154.

Pulles, T., van der Gon, H., Appelman, W., Verheul, M., 2012. Emission factors for heavy metals from diesel and petrol used in European vehicles. Atmos. Environ. 61, 641–651.

Querol, X., Alastuey, A., Moreno, T., Viana, M., Castillo, S., Pey, J., Rodríguez, S., Artiñano, B., Salvador, P., Sánchez, M., García Dos Santos, S., Herce Garraleta, M., Fernández– Partier, R., Moreno–Grau, S., Negral, L., Minguillón, M., Monfort, E., Sanz, M., Palomo–Marín, R., Pinilla–Gil, E., Cuevas, E., de la Rosa, J., Sánchez de la Campa, A., 2008. Spatial and temporal variations in airborne particulate matter (PM_{10} and $PM_{2.5}$) across Spain 1999–2005. Atmos. Environ. 42, 3964–3979.

Querol, X., Alastuey, A., Rodríguez, S., Plana, F., Ruiz, C., Cots, N., Massagué, G., Puig, O., 2001. PM_{10} and $PM_{2.5}$ source apportionment in the Barcelona Metropolitan area, Catalonia, Spain. Atmos. Environ. 35, 6407–6419.

Quiroz, W., Cortés, M., Astudillo, F., Bravo, M., Cereceda, F., Vidal, V., Lobos, M., 2013. Antimony speciation in road dust and urban particulate matter in Valparaiso, Chile: Analytical and environmental considerations. Microchem. J. 110, 266–272.

Ramírez, O., Sanchez de la Campa, A., Amato, F., Catacolí, R., Rojas, N., de la Rosa, J., 2018a. Chemical composition and source apportionment of PM_{10} at an urban background site in a high–altitude Latin American megacity (Bogota, Colombia). Environ. Pollut. 233, 142–155.

Ramírez, O., Sanchez de la Campa, A., de la Rosa, J., 2018b. Characteristics and temporal variations of organic and elemental carbon aerosols in a high–altitude, tropical Latin American megacity. Atmos Res. 210, 110–122.

Reimann, C., de Caritat, P., 2005. Distinguishing between natural and anthropogenic sources for elements in the environment: regional geochemical surveys versus enrichment factors. Sci. Total. Environ. 337, 91–107.

Robert, M., Kleeman, M., Jakober, Ch., 2007. Size and composition distributions of particulate matter emissions: Part 2–Heavy–duty diesel vehicles. J. Air & Waste Manage. Assoc. 57, 1429–1438.

Romero, M., Pinilla, R., Zafra, C., 2015. Temporal assessment of the heavy metals (Pb and Cu) concentration associated with the road sediment: Fontibón–Barrios Unidos (Bogotá D.C., Colombia). Ing. Univ. Bogotá 19(2), 315–333.

Rudnick, R., Gao, S., 2003. Composition of the Continental Crust. Treatise on Geochemistry 3, 1–64.

Saeedi, M., Li, L., Salmanzadeh, M., 2012. Heavy metals and polycyclic aromatic hydrocarbons: Pollution and ecological risk assessment in street dust of Tehran. J. Hazard. Mater. 227–228, 9–17.

Samiksha, S., Raman, R., Nirmalkar, J., Kumar, S., Sirvaiya, R., 2017. PM_{10} and $PM_{2.5}$ chemical source profiles with optical attenuation and health risk indicators of paved and unpaved road dust in Bhopal, India. Environ Pollut. 222, 477–485.

Schauer, J., Lough, G., Shafer, M., Christensen, W., Arndt, M., DeMinter, J., Park, J., 2006. Characterization of metals emitted from motor vehicles. Research Report 133. Health Effects Institute, Boton.

SDA – Secretaría Distrital de Ambiente, 2017. Informe anual de calidad del aire de Bogotá, 2016. SDA/Alcaldía Mayor de Bogotá, Bogotá.

SDA, 2016. Informe anual de calidad del aire de Bogotá, 2016. SDA/Alcaldía Mayor de Bogotá, Bogotá.

SDA, 2009. Elementos técnicos del Plan Decenal de Descontaminación de Bogotá. Parte 2: Inventario de emisiones provenientes de fuentes fijas y móviles. Alcaldía Mayor de Bogotá /Universidad de Los Andes, Bogotá.

SDM – Secretaría Distrital de Movilidad, 2017. Observatorio ambiental de Bogotá. Indicadores de movibilidad sostenible. Secretaría Distrital de Ambiente – SDA, Bogotá. http://oab.ambienteBogota.gov.co/es/temas?v=6&p=21 (accessed 04 February 2018) (In Spanish).

SDP – Secretaría Distrital de Planeación, 2017. Resumen del diagnóstico general. Plan de Ordenamiento Teritorial. Alcaldía Mayor de Bogotá, Bogotá.

Shen, Z., Sun, J., Cao, J., Zhang, L., Zhang, Q., Lei, Y., Gao, J., Huang, R., Liu, S., Huang, Y., Zhu, Ch., Xu, H., Zheng, Ch., Liu, P., Xue, Z., 2016. Chemical profiles of urban fugitive dust $PM_{2.5}$ samples in Northern Chinese cities. Sci. Total. Environ. 569–570, 619–626.

Shi, G., Chen, Z., Bi, C., Li, Y., Teng, J., Wang, L., Xu, S., 2010. Comprehensive assessment of toxic metals in urban and suburban street deposited sediments (SDSs) in the biggest metropolitan area of China. Environ. Pollut. 158 (3), 694–703.

Shi, G., Chen, Zh., Bi, Ch., Wang, L., Teng, J., Li, Y., Xu, Sh., 2011. A comparative study of health risk of potentially toxic metals in urban and suburban road dust in the most populated city of China.

Atmos. Environ. 45, 764–771.

Sjödin, Å., Ferm, M., Björk, A., Rahmberg, M., Gudmundsson, A., Swietlicki, E., Johansson, Ch., Gustafsson, M., Blomqvist, G., 2010. Wear particles from road traffic – a field, laboratory and modeling study. Final report B1830. IVL Swedish Environmental Research Institute Ltd., Göteborg.

Song, Q., Christiani, D., Wang, X., Ren, J., 2014. The global contribution of outdoor air pollution to the incidence, prevalence, mortality and hospital admission for chronic obstructive pulmonary disease: a systematic review and meta–analysis. Int. J. Environ. Res. Public Health 11(11), 11822–11832.

Strohbach, M., Arnold, E., Hasse, D., 2012. The carbon footprint of urban green space–A life cycle approach. Landsc. Urban Plan. 104(2), 220–229.

Tanner, P., Hoi–Ling, M., Yu, P., 2008. Fingerprinting metals in street dust in Beijing, Shanghai and Hong Kong. Environ. Sci. Technol. 42, 7111–7117.

Thorpe, A., Harrison, R., 2008. Sources and properties of non–exhaust particulate matter from road traffic: A review. Sci. Total Environ. 400, 270–282.

UNEP – United Nations Environment Programme, 2016. Global Environment Outlook (GEO–6). Regional assessment for Latin America and the Caribbean. United Nations Environment Programme, Nairobi.

Valotto, G., Rampazzo, G., Visin, F., Gonella, F., Cattaruzza, E., Glisenti, A., Formenton, G., Tieppo, P., 2015. Environmental and traffic–related parameters affecting road dust composition: A multi–technique approach applied to Venice area (Italy). Atmos. Environ. 122, 596–608.

Vargas, F., Rojas, N., Pachón, J., Russell, A., 2012. PM_{10} characterization and source apportionment at two residential areas in Bogota. Atmos. Pollut. Res. 3, 72–80.

Viana, M., Kuhlbusch, T., Querol, X., Alastuey, A., Harrison, R., Hopke, P., Winiwarter, W., Vallius, M., Szidat, S., Prévôt, A., Hueglin, C., Bloemen, H., Wåhlin, P., Vecchi, R., Miranda, A., Kasper–Giebl, A., Maenhaut, W., Hitzenberger, R., 2008. Source apportionment of particulate matter in Europe: a review of methods and results. J. Aerosol Sci. 39, 827–849.

Wahlin, P., Berkowicz, R., Palmgren, F., 2006. Characterisation of traffic–generated particulate matter in Copenhagen. Atmos. Environ. 40(12), 2151–2159.

Wang, G., Oldfield, F., Xia, D., Chen, F., Liu, X., Zhang, W., 2012. Magnetic properties and correlation with heavy metals in urban Street dust: A case study from the city of Lanzhou, China. Atmos. Environ. 46, 289–298.

Wang–Li, L., 2015. Insights to the formation of secondary inorganic $PM_{2.5}$: Current knowledge and future needs. Int. J. Agric. & Biol. Eng. 8(2), 1–13.

Wang, Y., Li, J., Cheng, X., Lun, X., Sun, D., Wang, X., 2014. Estimation of PM_{10} in the traffic–related atmosphere for three road types in Beijing and Guangzhou, China. J. Environ. Sci. 26, 197–

204.

Wei, B., Yang, L., 2010. A review of heavy metal contaminations in urban soils, urban road dusts and agricultural soils from China. Microchem. J. 94, 99–107.

Weinmayr, G., Romeo, E., De Sario, M., Weiland, S., Forastiere, F., 2010. Short–term effects of PM_{10} and NO_2 on respiratory health among children with asthma or asthma–like symptoms: A systematic review and meta–analysis. Environ. Health Perspect. 118(4), 449–457.

Wheida, A., Nasser, A., El Nazer, M., Borbon, A., El Ata, G., Wahab, M., Alfaro, S. 2018. Tackling the mortality from long–term exposure to outdoor air pollution in megacities: Lessons from the Greater Cairo case study. Environ. Res. 160, 223–231.

WHO – World Health Organization, 2016. World Health Statistics 2016. WHO, Geneva.

Wongphatarakul, V., Friedlander, S., Pinto, J., 1998. A comparative study of $PM_{2.5}$ ambient aerosol chemical databases. Environ. Sci. Technol. 32, 3926–3934.

Wua, J., Jiang, X., Wheatley, A., 2009. Characterizing activated sludge process effluent by particle size distribution, respirometry and modeling. Desalination 249, 969–975.

Yongming, H., Peixuan, D., Junji, C., Posmentier, E., 2006. Multivariate analysis of heavy metal contamination in urban dusts of Xi'an, Central China. Sci. Total. Environ. 355, 176–186.

Zafra, C., Santamaría, D., Torres, C., 2015. Climatic analysis of heavy metal concentration associated with urban road–deposited sediment. Rev. salud pública 17(3), 351–364.

Zhang, Ch., Qiao, Q., Appel, E., Huang, B., 2012. Discriminating sources of anthropogenic heavy metals in urban street dusts using magnetic and chemical methods. J. Geochem. Explor. 119–120, 60–75.

Zhang, Q., Shen, Z., Cao, J., Ho, K., Zhang, R., Bie, Z., Chang, H., Liu, S., 2014. Chemical profiles of urban fugitive dust over Xi'an in the south margin of the Loess Plateau, China. Atmos. Pollut. Res. 5, 421–430.

Zhao, P., Feng, Y., Zhu, T., Wu, J., 2006. Characterizations of resuspended dust in six cities of North China. Atmos. Environ. 40, 5807–5814.

Zoller, W., Gladney, E., Duce, R., 1974. Atmospheric concentrations and sources of trace metals at the South Pole. Science 183, 199–201.